

Improvement of femtosecond SPPs imaging by two-color laser photoemission electron microscopy

Chun-Lai Fu(付春来), Zhen-Long Zhao(赵振龙), Bo-Yu Ji(季博宇)†, Xiao-Wei Song(宋晓伟)‡, Peng Lang(郎鹏), and Jing-Quan Lin(林景全)

Citation: Chin. Phys. B, 2022, 31 (**10**): 107103. DOI: 10.1088/1674-1056/ac6ede
Journal homepage: http://cpb.iphy.ac.cn; http://iopscience.iop.org/cpb

What follows is a list of articles you may be interested in

Light focusing in linear arranged symmetric nanoparticle trimer on metal film system

Yuxia Tang(唐裕霞), Shuxia Wang(王蜀霞), Yingzhou Huang(黄映洲), and Yurui Fang(方蔚瑞)
Chin. Phys. B, 2022, 31 (**1**): 017303. DOI: 10.1088/1674-1056/ac20c3

Collective excitations and quantum size effects on the surfaces of Pb(111) films: An experimental study

Yade Wang(王亚德), Zijian Lin(林子荐), Siwei Xue(薛思玮), Jiade Li(李佳德), Yi Li(李毅), Xuetao Zhu(朱学涛), and Jiandong Guo(郭建东)
Chin. Phys. B, 2021, 30 (**7**): 077308. DOI: 10.1088/1674-1056/abfbcd

Quantifying plasmon resonance and interband transition contributions in photocatalysis of gold nanoparticle

Liang Dong(董亮), Chengyun Zhang(张成云), Lei Yan(严蕾), Baobao Zhang(张宝宝), Huan Chen(陈环), Xiaohu Mi(弥小虎), Zhengkun Fu(付正坤), Zhenglong Zhang(张正龙), and Hairong Zheng(郑海荣)
Chin. Phys. B, 2021, 30 (**7**): 077301. DOI: 10.1088/1674-1056/abfa0c

Tunable localized surface plasmon resonances in one-dimensional h-BN/graphene/h-BN quantum-well structure

Kaibiao Zhang(张开彪), Hong Zhang(张红), Xinlu Cheng(程新路)
Chin. Phys. B, 2016, 25 (**3**): 037104. DOI: 10.1088/1674-1056/25/3/037104

Effects of shape and dopant on structural, optical absorption, Raman, and vibrational properties of silver and copper quantum clusters： A density functional theory study

Li Wei-Yin, Chen Fu-Yi
Chin. Phys. B, 2014, 23 (**11**): 117103. DOI: 10.1088/1674-1056/23/11/117103

Improvement of femtosecond SPPs imaging by two-color laser photoemission electron microscopy

Chun-Lai Fu(付春来), Zhen-Long Zhao(赵振龙), Bo-Yu Ji(季博宇)[†], Xiao-Wei Song(宋晓伟)[‡], Peng Lang(郎鹏), and Jing-Quan Lin(林景全)

School of Physics, Changchun University of Science and Technology, Changchun 130022, *China*

(Received 2 March 2022; revised manuscript received 6 May 2022; accepted manuscript online 12 May 2022)

Clear imaging of surface plasmon polaritons (SPPs) is a prerequisite for SPPs-based applications. In this work, we demonstrate an improvement of near-field imaging of SPPs via directly comparing the visibility of the photoemission electron microscopy (PEEM) image of SPPs under one- and two-color laser excitation (also known as one- or two-color laser PEEM). By measuring the photoelectron yield and the contrast of the interference fringes of SPPs, we demonstrate that in addition to enhancing the photoemission yield, two-color laser PEEM can significantly improve the contrast between bright and dark fringes (nearly 4 times higher than that of one-color laser case). By recording the nonlinear order of the photoelectrons ejected from the bright and dark fringes, respectively, the underlying mechanism for the improved visibility is revealed. In addition, the influences of the polarization direction of 400-nm laser on the PEEM images of the SPPs with different wave vector directions are shown. These results can provide technical support for the development of SPPs-based communication devices and catalysis.

Keywords: surface plasmon polaritons, photoemission electron microscopy, near-field imaging

PACS: 71.45.Gm, 73.20.Mf **DOI:** 10.1088/1674-1056/ac6ede

1. Introduction

Surface plasmon polaritons (SPPs), an electromagnetic wave transmitted at the metal–dielectric interface can propagate nearly millimeters with the excitation by near-infrared photons,[1] and can be used in nanoscale plasmon lasers,[2] local optical traps,[3,4] plasmon waveguides,[3,5–9] sensor,[10] and metamaterial,[11] and has strong potential applications in the next generation of highly integrated nano-photoelectron devices.[12–16]

Owing to the subwavelength localization of SPPs, it is generally an important prerequisite to reveal the physical nature of plasmon fields by using a microscopy with nanoscale spatial-resolution. The imaging of SPPs can be carried out through optical fluorescence microscope, fluorescence labeling,[16] or visualized by scanning near-field optical microscopy (SNOM) with higher spatial resolution (about 10 nm).[17] Photoemission electron microscopy (PEEM) with a lateral resolution similar to SNOM, a fast acquire rate, an attosecond temporal resolution accessibility and without being affected by the probe tip, has been utilized to characterize the transmission or localization of plasmons by observing the interference fringe or the hot spots.[18–20]

Despite the fact that the near-field image of SPPs by PEEM can be obtained via one-color ultrafast laser illumination, the electrons within the sample undergo a high-order nonlinear process to produce photoemission under infrared ultrafast laser excitation due to the relatively high work function of the sample (*e.g.* 4.6 eV–5.2 eV for gold). In this regard, an extremely strong incident laser intensity is required for necessary image brightness. Nevertheless, this will easily result in melting or reconstruction of the sample during PEEM measurement. To avoid the above limitation, an atomic thick layer of alkali metal (such as cesium) can be deposited on the sample surface to lower the work function of the sample, reduce the nonlinear order of the multi-photon photoemission process and thereby enhance the brightness of PEEM image.[13,21,22] However, the drawback of this method is that the deposition of alkali metal will lead the sample difficult to be used for potential practical application since it undoubtedly will limit the reusability of the sample once exposed to air due to the highly reactivity of alkali metal.

In recent years, two-color laser PEEM scheme, which can reduce the nonlinear order of the emitted photoelectron via the two-color ultrafast laser illumination, has been utilized to obtain the near-field image and the group/phase velocity of SPPs without the risk of damaging the sample.[23–27] Nevertheless, a systematical evaluation of the two-color laser PEEM image method, especially a direct comparation between one-/two-color laser PEEM (include the image brightness and the contrast of the SPPs fringes, *etc.*) is, to the best of our knowledge, rarely reported.

In this paper, a direct and comprehensive comparation between one-/two-color laser excited PEEM image of SPPs (including the brightness and the contrast of SPPs) is carried out.

[†]Corresponding author. E-mail: jiboyu@cust.edu.cn
[‡]Corresponding author. E-mail: songxiaowei@cust.edu.cn

© 2022 Chinese Physical Society and IOP Publishing Ltd

The results show that the two-color laser excitation can increase the brightness of the PEEM image via enhancing the photoelectron yield, which can realize the imaging of weakly excited SPPs. More importantly, it is found that the contrast of SPPs fringes under two-color laser PEEM scheme can be significantly increased (up to 4 times in our case) in comparison with that under one-color laser excitation. By recording the nonlinear order of the photoelectrons emitted from the bright and dark fringe, respectively, the underlying physical mechanism of the improved visibility of SPPs is revealed by using two-color laser scheme. We attribute this result to the higher opening degree of the quantum channel at the position of the bright fringe than that of dark fringe. In addition, the effects of polarization angle of second harmonic laser (400 nm in this case) on the PEEM image of SPPs with different wave vector directions are presented as well.

2. Experimental setup

A 100-nm-thick Au film was evaporated onto an indium tin oxide coated clean silica substrate, and a rectangle groove structure with a size of 10 μm×1 μm was etched by focused ion beam lithography. The PEEM image of the groove structure under mercury lamp illumination is shown in the inset of Fig. 1(a). Figure 1(b) shows the schematic diagram of the experiment. The SPPs were excited by a mode-locked titanium-sapphire laser with a central wavelength of 800 nm (Coherent, Mira 900, 76-MHz repetition rate, 150-fs pulse width). The laser pulse is split into two beams within a Mach–Zehnder interferometer equipped with a piezoelectric translation platform, one of which produces the second harmonic (400 nm) laser from a BBO crystal. The power and polarization angle for each of these two lasers beams can be adjusted by using two independent neutral density attenuators (which ranges from 30 mW to 70 mW for 800-nm pulses and from 2 mW to 9 mW for 400-nm pulses) and corresponding half wave plates, respectively. Two pulses went through two flanges of the PEEM, and then focused at the same position on the sample surface at an incident angle of 65° relative to the surface normal. The focal spot sizes of the two pulses were adjusted to basically the same size: about 30 μm×20 μm, by the focusing lens. The PEEM is used to collect the photoemission electrons ejected from the sample, and to achieve direct imaging of the near-field interference fringes of SPPs. Figure 1(c) shows the relative time-delay-dependent photoemission electron yield which presents a peak at 0 fs. Meanwhile, the 0-fs time delay will be adopted in subsequent studies. The inset in Fig. 1(c) shows the two-color PEEM image of the SPPs at the time delay of 0 fs. On account of the extremely strong photoelectron emission from the edge of groove structure due to the excitation of localized surface plasmons, the groove structure is moved out of the field of view to avoid saturation of the PEEM image.

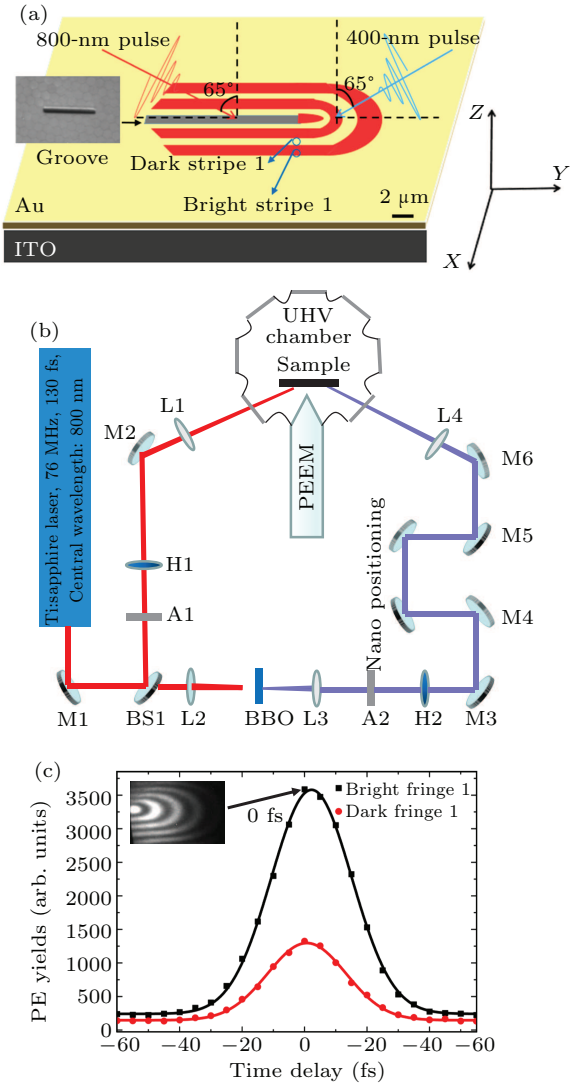


Fig. 1. (a) Schematic diagram of experiment, with the inset showing one-photon PEEM image of sample diagram under illumination of mercury lamp; (b) experimental set up of two-color laser PEEM experimental scheme, where M1–M5 are silver mirrors, BS1 is beam splitter, L1–L4 correspond to convex lens, A1 and A2 are neutral attenuation plates, and H1, H2 are both half plate for 800-nm and 400-nm pulses, respectively; (c) hotelectron yield *versus* relative time delay between two color laser pulses for dark strip 1 and bright strip 1, with inset showing two-color laser PEEM image of SPPs at a time delay of laser pulse at 0 fs.

3. Results and discussion

Figure 2(a) shows the one-color PEEM images of the sample irradiated by a single 55-mW, 800-nm femtosecond laser pulse at three different polarization angles. Distinct interference fringes can be observed under a laser polarization angle of 0° (p-polarization). Nevertheless, no distinct fringes can be seen under laser polarization angle of 90° (s-polarization). This is attributed to the ineffective excitation of SPPs under s-polarization laser illumination. Namely, it is hard for conventional one-color PEEM to clearly image the SPPs with weak excitation. Figure 2(b) shows the two-color PEEM images with an additional 2-mW, 400-nm femtosecond laser beam (p-

polarization). These results show that the brightness of image is significantly enhanced with respect to one-color laser PEEM scheme for the given polarization directions of 800 nm. Specifically, when the polarization angle of 800-nm laser pulse is tuned to 90°, SPP interference fringes can also be distinguished. By extracting the photoelectron yield at the same position (as shown in Figs. 2(a) and 2(b)) of the bright fringe under one-/two-color laser conditions, the 800-nm laser polarization angle-dependent photoemission yield is shown in Fig. 2(c). It can be seen that by introducing a 400-nm laser pulse, the photoemission yield of SPP interference fringes can effectively increase by nearly two times as great as that of one-color laser scheme.

It should be understood that the increase of the photoelectron yield from the sample under two-color laser excitation cannot be directly equivalent to the improvement of the image visibility. The contrast between the bright and dark fringes is an important parameter to evaluate the visualization of the SPP. The contrast between the SPP fringes under one- and two-color laser PEEM case should be considered simultaneously to evaluate the visibility of the PEEM image more accurately. To this end, we further extract the photoemission yield from the adjacent dark fringe, and calculate the contrast from the following formula:

$$K = \frac{I_{\max} - I_{\min}}{I_{\max} + I_{\min}}, \tag{1}$$

where $I_{\max}$ and $I_{\min}$ correspond to the photoemission yield of the bright and dark fringe (marked in Fig. 1(a)), respectively. Figure 2(d) shows the 800-nm laser polarization angle-dependent contrast under one-/two-color laser excitation condition, respectively. Firstly, it can be seen that the fringe contrast gradually decreases with the increase of polarization angle of 800-nm incident laser. More importantly, we should mention that the contrast of interference fringes obtained under two-color laser excitation condition is significantly higher than that under one-color laser excitation. Specifically, with 40° polarization angle of 800-nm laser, the fringe contrast obtained under two-color laser excitation is 0.22 which is about 4 times higher than that under one-color laser excitation. These results corroborate that in addition to observing weakly excited SPPs by enhancing the image brightness, the two-color laser scheme can enhance the visibility of the PEEM image of SPPs via increasing the contrast between the bright fringe and the dark fringe in comparison with the one-color laser scheme. It should be noted that the bright fringes under one-color excitation are almost invisible (accompanied with the contrast close to 0), with the 800-nm laser's polarization angle being greater than 50°. We, therefore, do not make quantitative comparison of contrast between one-color case and two-color case under this condition.

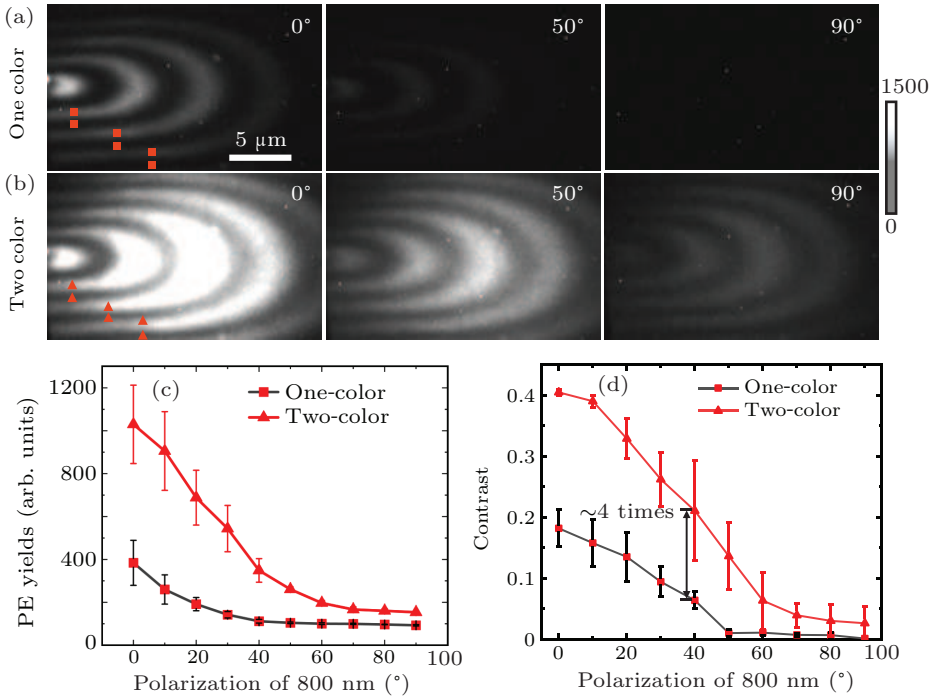


Fig. 2. PEEM images of SPP interference fringes obtained by (a) single 800-nm laser pulse and (b) two-color (400 nm+800 nm) laser pulse with 800-nm laser pulse's polarization angle of 0°, 50°, and 90°; (c) photoemission electron yields and (d) the contrast of SPPs fringes *versus* 800-nm laser pulse's polarization angle. The error bars in panels (b) and (c) are made based on three different SPP fringe groups for one-color laser case (marked by the red rectangles in panel (a)) and for two-color laser case (marked by the red triangles in panel (b)), respectively.

To further reveal the underlying mechanism for the visibility improvement of the PEEM image of SPPs under two-color laser excitation, the photoemission electron yields of bright and dark fringes of SPPs under the power of 800-nm and 400-nm laser are extracted, the results are shown in Fig. 3. The relationship between photoemission electron yield Y and laser

intensity I can be presented by the following expression:[28]

$$Y \propto I^n, \tag{2}$$

where n represents the nonlinear order of the photoemission. Figure 3(a) shows the 800-nm laser (p-polarization) power-dependent photoelectron yield from bright and dark fringes of SPPs under one-color laser excitation. The nonlinear order of the photoelectrons emitted from the bright fringe and the dark fringe are 3.61 ± 0.09 and 3.2 ± 0.27, respectively, indicating a 4-photon photoelectron emission process. The 800-nm laser (p-polarization) power-dependent photoelectron yield from bright fringe and dark fringe under two-color laser excitation are shown in Fig. 3(b). In this case, the power of 400-nm laser pulse (p-polarization) is fixed at 3 mW. It can be seen that with the assistance of 400-nm laser, the nonlinear order of bright fringe and dark fringe decrease to 1.88 ± 0.15 and 2.11 ± 0.24, respectively. More importantly, we should note that the nonlinear order variation between bright fringe and dark fringe is different: for the bright fringe, the nonlinear order decreases from 3.61 to 1.88 (with a decrement of 1.73); for the dark fringe, the nonlinear order decreases from 3.2 to 2.11 (with a decrement of 1.09). It is known that the photoemission electron under two-color femtosecond laser excitation can be treated as a process of the opening of two-color quantum channel,[29] and a larger opening degree of the two-color quantum channel will result in the drastic reduction of the nonlinear order of photoelectrons accompanied with the significant increase of the photoemission yields.[23] The different nonlinear order variations at bright fringe and dark fringe clearly demonstrate that the visibility improvement of the PEEM image under two-color laser excitation results from the different opening degrees of the quantum channel spatially: the bright fringe corresponds to a higher opening degree of the quantum channel. This can be explained as follows: a 400-nm laser beam dominates the photoelectron emission in the dark fringe formed by the destructive interference between SPPs and 800-nm pump pulse, therefore the condition of the effective opening of the two-color channel is weaker than in the case of the bright fringe.[23–25] To further confirm our deduction, the 400-nm laser (p-polarization) power-dependent photoemission yields, with the power of 800-nm laser (p-polarization) fixed at 32mW, are shown in Fig. 3(c). The result shows that the nonlinear order of bright fringe (1.23 ± 0.09) is still lower than that of dark fringe (1.38 ± 0.11). Similarly, this result demonstrates that there exists a higher opening degree for the bright fringe than that for the dark one. In short, the physical mechanism of the enhanced contrast between the bright fringe and the dark fringe under two-color laser excitation arises from the spatially different opening degrees of the quantum channel between the bright fringe and the dark fringe.

Furthermore, we also obtain the contrast of SPP fringes at different 800-nm laser power values (32 mW to 48 mW, corresponding to Figs. 3(a) and 3(b)) for both the two-color laser excitation case and the one-color laser excitation case, which is not shown here. It is found that the contrast of the one-color laser case and two-color laser case increase with the further enhancement of the power of 800-nm laser, and the contrast under the two-color laser case is always higher than that under the one-color laser case. Note that the above results are obtained in zone 1 (see Fig. 4(a) for zone 1), and measurements in the zone 2 give very similar results, *i.e.*, the conclusions obtained from zone 1 are applicable to the case of zone 2.

To further demonstrate that the 400-nm laser pulse plays a role in enhancing the visibility of the SPPs, we display the 400-nm laser power-dependent contrast in the two-color laser pulse's illumination scheme with 800-nm laser power of 50 mW. As shown in Fig. 3(d), with the increase of 40-nm power from 2 mW to 10 mW, the contrast of the fringe first shows a trend of increase, and then gradually decreases. This can be attributed to the fact that there is an optimal power ratio between 400-nm laser pulse and 800-nm laser pulse to maximize the opening degree of quantum channel.[23] While the increase of 400-nm laser power can enhance the intensity of bright fringes, the dark fringe and background intensity can increase simultaneously as shown in Fig. 3(c). Therefore, the contrast of the fringe can be observed to decrease with 400-nm laser power increasing. The result of Fig. 3(d) shows that the photoemission from 400-nm laser exerts an important influence on the contrast of the fringes.

In the above research, we have directly compared the visibilities of the PEEM image of SPPs under one- and two-color laser excitation and found that, in addition to the enhancement of the photoemission yield, two-color PEEM can significantly improve the contrast between bright fringe and dark fringe (nearly 4 times higher than that of one-color case) and therefore enhancing the visibility. Next, the influence of 400-nm laser polarization angle (the 800-nm laser pulse is p-polarized one) on the PEEM image of SPPs is explored. Here, SPPs within different zones near the structure (marked by zone 1 and zone 2 in Fig. 4(a)), which corresponds to different wave vector directions respectively, are selected, and their schematic diagrams are shown in Fig. 4(a). The SPPs in zone 2 are excited by shorter edge of the groove which is along the x axis. The in-plane component (E_{SL} as depict in Fig. 4(a)) of the SPPs selected in zone 2 is parallel to the electric field of the 800-nm laser, projected onto the gold surface. This will give a long overlapping time between the SPPs and the incident laser. In contrast, the SPPs in zone 1 are excited by longer edge of the grove which is along the y axis. The E_{SL} component of SPPs in zone 1 intersects with the electric field of the

800-nm laser projected onto the gold surface. In this case, the overlapping time between the SPPs and the incident laser in zone 1 is shorter than in the case in zone 2. As a result, the fringe width in zone 1 is narrower than the one in zone 2.[18] It is needed to mention that as the SPPs in zone 2 correspond to a longer overlapping time and a higher coupling efficiency between laser and SPPs, a commonly used excitation framework should be used in the study and utilization of SPPs.[25,30] In contrast, owing to the narrower fringe period, the SPPs in zone 1 have been found recently to be conducive to the direct characterization of SPP properties and to the development of various SPPs-based applications.[18,31–34]

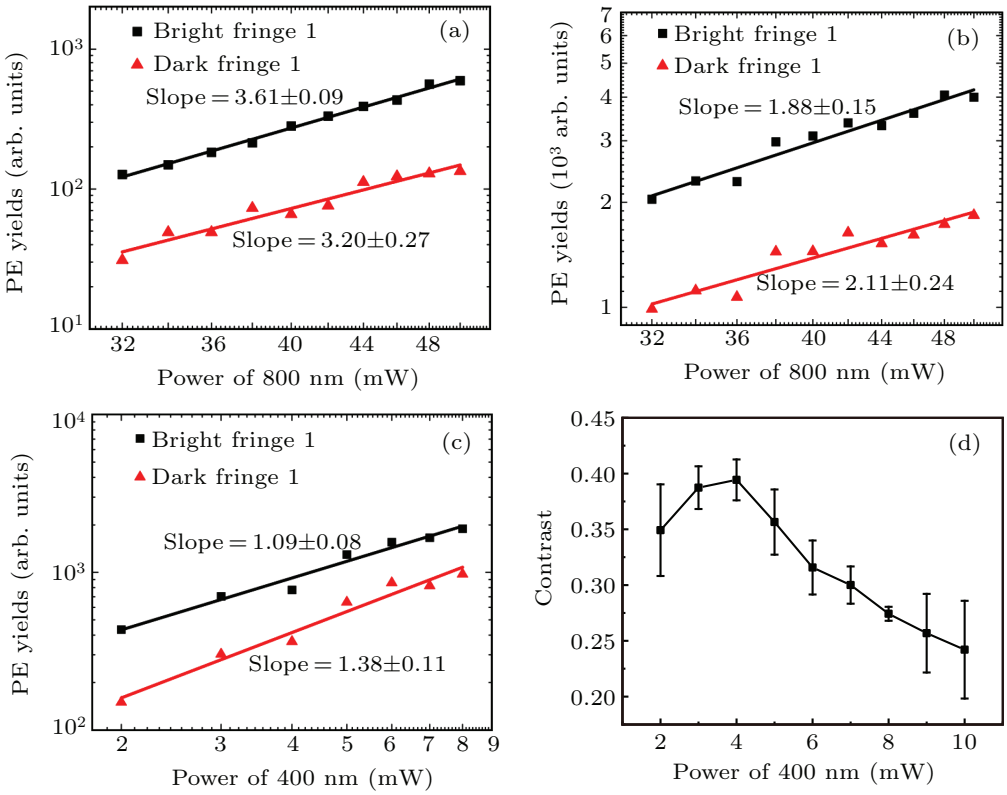


Fig. 3. Plots of photoemission electron yield *versus* 800-nm laser power under (a) one-color laser excitation and (b) two-color laser excitation; (c) plots of photoemission electron yield *versus* 400-nm laser power under two-color laser excitation. All photoelectron yields have subtracted background intensity. Meanwhile, the photoelectron yield generated from the isolated laser pulses with fixed intensity under the two-color condition is also deducted. (d) Plot of contrast *versus* 400-nm laser power in zone 1 under two-color (400 nm+800 nm) laser pulses illumination. The error bars are made based on three different SPP fringe groups (marked by red triangles in Fig. 2(b)).

The photoemission electron yields of bright fringe and dark fringe related with the polarization angle of 400-nm laser is shown in Fig. 4(b). From this figure it follows that the photoemission yields of bright fringe and dark fringe of SPPs in both zone 1 and zone 2 decrease rapidly with the increase of polarization angle of 400-nm laser pulse from 0° to 90°. More importantly, it can be seen that the variation trends of the curves of polarization angles of 400-nm laser *versus* photoemission yield curves for the SPPs with different wave vector directions are basically consistent with each other. We attribute this result to the following possible reasons: (i) the SPPs induced by 800-nm laser correspond to an incoherent superposition with 400-nm laser; (ii) since SPPs-induced photoelectrons are dominated by out-of-plane component E_{ST} as depicted in Fig. 4(a),[30] the direction of E_{ST} in zone 1 is identical to that in zone 2, therefore the response of the photoelectrons ejected from zone 1 to the polarization direction of 400-nm laser is the same as that from zone 2. Moreover, the contrast of PEEM image of SPPs in the two zones related with the polarization angle of 400-nm laser is also investigated. We extract the contrasts from three different groups of bright fringes and dark fringes in zone 1 and zone 2 as marked in the inset in Fig. 4(c), respectively, and the results are displayed in Fig. 4(c). From this figure it follows that the contrast of SPP fringes in each of zone 1 and zone 2 shows a slow decreasing trend with turning polarization angle of 400-nm laser increasing from 0° to 90°, even though the fringe periods in the two zones are quite different. In addition, it is noted that the variation in the contrast for zone 1 in Fig. 4(c) and that in Fig. 2(d) generally follow the same trend but have some differences in decreasing rate with the laser polarization angle increasing for the two-color laser scheme under the same polarization condition. This phenomenon should result from the different laser wavelengths corresponding to the polarization-dependent measurement in Figs. 4(c) and 2(d). Moreover, it should be noted that the laser power corresponding to Fig. 4(c) is different from that corresponds to Fig. 2(d).

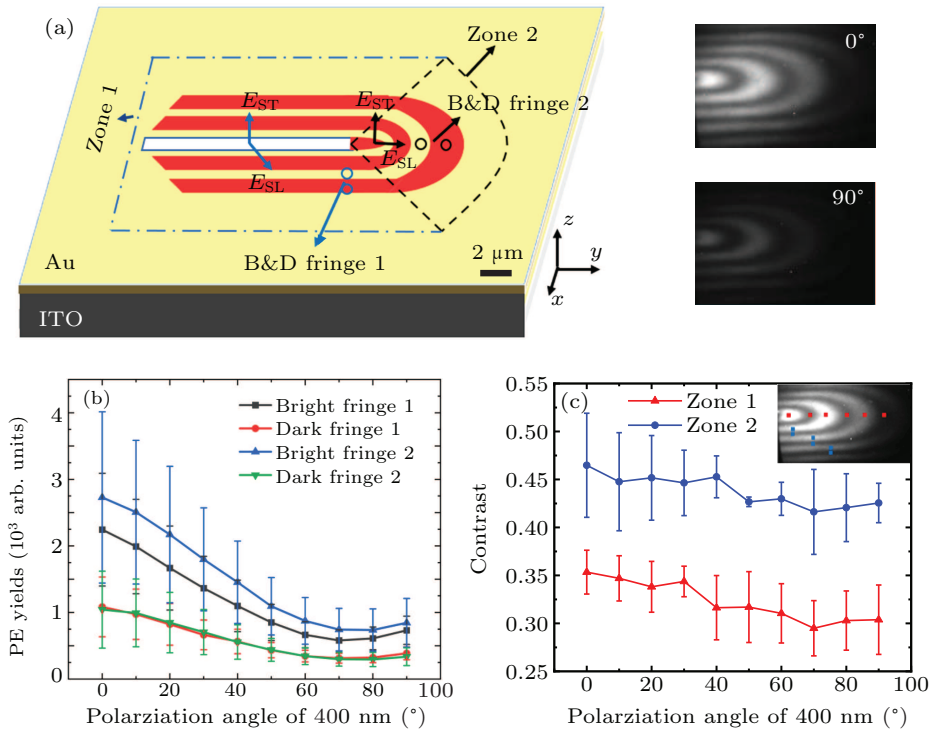


Fig. 4. (a) Schematic diagram of electric field components of SPPs on the surface of gold film. E_{ST} and E_{SL} are the SPPs' electric field components perpendicular and parallel to the gold surface, respectively. The two insets show PEEM image of SPPs obtained under two-color excitation with 400-nm polarization angle of 0° (upper) and 90° (lower), respectively; (b) plots of photoemission electron yield *versus* polarization angle of 400-nm laser at bright fringes 1 and 2 and dark fringes 1 and 2; (c) plots of contrast of SPPs' fringes *versus* polarization angle of 400-nm laser for zone 1 and zone 2, respectively. The error bars in panels (b) and (c) are made based on three different SPP fringe groups in zone 1 (marked by red triangles) and in zone 2 (marked by blue circles) in inset, respectively.

4. Conclusions

We directly and comprehensively compared the brightness (photoelectron yield) and the contrast of the PEEM image of the SPPs exited from an etched groove structure in gold film under one-color laser photoemission electron microscopy with those under two-color laser photoemission electron microscopy. The results show that in addition to enhancing the photoemission yields that can be used to obtain the image of weakly excited SPPs, two-color laser excitation can significantly improve the visibility of the PEEM image due to the enhanced contrast between bright fringe and dark fringe in comparison with one-color laser excitation (up to about 4 times). By recording the nonlinear order of the photoelectrons ejected from the bright fringes and dark fringes, respectively, the underlying mechanism responsible for improving the visibility is revealed: for the two-color excitation, the opening degree of the two-color quantum channel corresponding to the bright fringes is higher than the one corresponding to the dark fringes. Moreover, it is found that the variation trends of the curves of 400-nm polarization angle *versus* photoemission yield for the SPPs with different wave vector directions are basically consistent with each other. These results may deepen the understanding of the mechanism of two-color laser PEEM and will help broaden the scope of application of SPPs.

Acknowledgements

Project supported by the National Natural Science Foundation of China (Grant Nos. 62005022 and 12004052), the Fund from the Jilin Provincial Key Laboratory of Ultrafast and Extreme Ultraviolet Optics, China (Grant No. YDZJ202102CXJD028), the Fund from the Department of Science and Technology of Jilin Province, China (Grant Nos. 20200201268JC and 20200401052GX), the "111" Project of China (Grant No. D17017), and the Fund from the Ministry of Education Key Laboratory for Cross-Scale Micro- and Nano-Manufacturing, Changchun University of Science and Technology, China.

References

[1] Brongersma M L and Shalaev V M 2010 *Science* **328** 440
[2] Berini P and Leon I D 2012 *Nat. Photon.* **6** 16
[3] Maier S A and Atwater H A 2005 *J. Appl. Phys.* **98** 10
[4] Benson O 2011 *Nature* **480** 193
[5] Barnes W L, Dereux A and Ebbesen T W 2003 *Nature* **424** 824
[6] Berini P, Charbonneau R and Lahoud N 2005 *J. Appl. Phys.* **98** 043109
[7] Ozbay E 2006 *Science* **311** 189
[8] Gramotnev D K and Bozhevolnyi S I 2010 *Nat. Photon.* **4** 83
[9] Fu P B and Chen Y G 2022 *Chin. Phys. B* **31** 014216
[10] Hu L X, He Z Q, Hu M and Liu S G 2021 *Chin. Phys. B* **30** 084102
[11] Suo P, Mao L and Xu H 2020 *Chin. Phys. Lett.* **30** 017801
[12] Wei H, Pan D, Zhang S, Li Z, Li Q, Liu N, Wang W and Xu H 2018 *Chem. Rev.* **118** 2882
[13] Lemke C, Schneider C, Leißner T, Bayer D, Radke J W, Fischer A, Melchior P, Evlyukhin A B, Chichkov B N, Reinhardt C, Bauer M and Aeschlimann M 2013 *Nano Lett.* **13** 1053

[14] Spektor G, Kilbane D, Mahro A K, G. Frank B. Ristok S, Gal L, Kahl P, Podbiel D, Mathias S, Giessen H F, Meyer zu Heringdorf F J, Orenstein M and Aeschlimann M 2017 *Science* **355** 1187

[15] Joly A G, Gong Y, El-Khoury P Z and Hess W P 2018 *J. Phys. Chem. Lett.* **9** 6164

[16] Wild B, Cao L, Sun Y, Khanal B P, Zubarev E R, Gray S K, Scherer N F and Pelton M 2012 *ACS Nano* **6** 472

[17] Wang Q, Bu J and Yuan X 2010 *Opt. Express* **18** 2662

[18] Qin Y, Song X, Ji B Xu Y and Lin J 2019 *Opt. Lett.* **44** 2935

[19] Yang J, Sun Q, Yu H, Ueno K, Misawa H and Gong Q 2017 *Photon. Res.* **5** 187

[20] Liu W, Yu H, Li Y, Hu A, Wang j, Lu G, Li X, Yang H, Dai L, Wang S and Gong Q 2021 *Nano Lett.* **21** 2932

[21] Kirschbaum P, Buckanie N M and Heringdorf F J 2012 *Plasmonics* **7** 229

[22] Leißner T, Thilsing-Hansen K, Lemke C, Jauernik S, Kjelstrup-Hansen J, Bauer M and Rubahn H G 2012 *Plasmonics* **7** 253

[23] Ji B, Song X, Dou Y, Tao H, Gao H, Hao Z and Lin J 2018 *New J. Phys.* **20** 073031

[24] Hu H, Qin Y, Lang P, Song X, Ji B and Lin J 2022 *Opt. Laser Technol.* **146** 107538

[25] Zhao Z, Lang P, Qin Y Ji B, Song X and Lin J 2020 *Opt. Express* **28** 19023

[26] Shibuta M, Eguchi T and Nakajima A 2013 *Plasmonics* **8** 1411

[27] Crampton K T, Joly A G and El-Khoury P Z 2019 *J. Phys. Chem. Lett.* **10** 5694

[28] Gong Y, Joly A G, Hu D and Hess W P 2015 *Nano Lett.* **15** 3472

[29] Förster M, Paschen T, Krüger M, Lemell C, Wachter G, Libisch F, Madlener T, Burgdörfer J and Hommelhof P 2016 *Phys. Rev. Lett.* **117** 217601

[30] Yamagiwa K, Shibuta M and Nakajima A 2017 *Phys. Chem. Chem. Phys.* **19** 13455

[31] Qin Y, Xu Y, Ji B, Song X and Lin J 2022 *Appl. Phys. B* **128** 1

[32] Gong Y, Joly A G, El-Khoury P Z and Hess W P 2017 *J. Phys. Chem. Lett.* **8** 49

[33] Qin Y, Ji B, Song X and Lin J 2021 *Photon. Res.* **9** 514

[34] Podbiel D, Kahl P, Makris A, Frank B, Sindermann S, Davis T J, Giessen H, Hoegen M H and Meyer zu Heringdorf F J 2017 *Nano Lett.* **17** 6569